Polar Meteorol. Glaciol., **18**, 82–95, 2004

Effects of intraseasonal variations of the Arctic Oscillation on the Barents Sea

Bingyi Wu[1]*, Jia Wang[2] and Renhe Zhang[1]

[1]*Chinese Academy of Meteorological Sciences, Beijing, 100081, China*
[2]*International Arctic Research Center, University of Alaska Fairbanks, Fairbanks, 99775, Alaska, U.S.A.*
**Corresponding author. E-mail: wby@cams.cma.gov.cn*

(Received May 27, 2004; Accepted August 10, 2004)

Abstract: This paper investigates possible connections among the wintertime Arctic Oscillation (AO), North Atlantic water inflow into the Barents Sea, and sea ice and sea water temperature in the Barents Sea on monthly to seasonal time scales using a coupled sea-ice-ocean model. The forcing is from winters with large anomalies of the AO. The inflow of the North Atlantic water into the Barents Sea forced by significantly different wind stresses over the area south of the Barents Sea shows a close relation to the AO only during the AO high-phase periods rather than during the low-phase periods. The responses to forcing by the opposite phases of the AO differ substantially in surface and subsurface water temperature of the Barents Sea. The positive phase of the AO raises subsurface water temperature in the Barents Sea, with concurrent surface cooling in the western and central Barents Sea. One exception is in the eastern Barents Sea where the surface water temperature is higher during the positive phase than during the negative phase. The enhanced net inflow of warmer Atlantic water into the Barents Sea causes decrease of sea ice.

key words: Arctic Oscillation, North Atlantic water, Barents Sea, sea ice, sea water temperature

1. Introduction

The Barents Sea is situated between 70° and 80°N on the North European continental shelf, and is a relatively shallow marginal sea of the Arctic Ocean with an average depth of 230 m. Its topographical features include Spitsbergen to the North, and NovayaZemlya to the east. Ice-cover extends over 1/3 to 2/3 of the Barents Sea and varies considerably during the year and inter-annually.

As Ikeda (1990) suggested, the most crucial area of ocean-ice-air feedback may be the Barents Sea, which is the northernmost ice-free area. Sea ice variations in the Barents Sea on interannual and decadal time scales show close relationships with the atmospheric circulation and the North Atlantic water inflow, and sea ice variations could produce dynamic feedback to the atmosphere (Ikeda 1990; Gao and Wu, 1998; Dickson *et al*., 2000; Wu *et al*., 2000, 2004). Recent research shows that sea ice variations in the Barents Sea can produce local and remote influences on the atmospheric circulation during the winter season (Deser *et al*., 2004; Alexander *et al*., 2004).

Because of limited observations in the Arctic Ocean, we only have a rudimentary understanding of mechanisms involving these complicated interaction processes. Consequently, a coupled sea ice-ocean model can be a powerful tool to explore interactions between Arctic sea ice and the ocean, and how the Arctic Ocean responds to atmospheric forcing. Through numerical simulation, Proshutinsky and Johnson (1997) revealed that wind-driven motion in the central Arctic alternates between anticyclonic and cyclonic circulation, with each regime persisting for 5–7 years, and the shift from one regime to another is forced by changes in the location and intensity of the Icelandic Low and the Siberian High. Zhang, J. *et al*. (1998) investigated the possible reason for the warming of the Arctic Ocean, and they attributed those changes to a sustained increase of the Atlantic inflow both via Fram Strait and through the Barents Sea, which is in agreement with the conclusions of Häkkinen and Geiger (2000).

Based on observations, Dickson *et al*. (2000) and Wu *et al*. (2000) suggested that the North Atlantic Oscillation (NAO) directly affects the North Atlantic water inflow into the Barents Sea on interannual time scales. The North Atlantic water inflow further influences sea ice extent in the Barents Sea. Our motivation is the fact that there is large intraseasonal and interannual variation in the AO, even during longer periods of a preferred phase of the AO. The responses to the intraseasonal variations of the AO are largely unexplored in regions such as the Barents Sea, an important pathway between the North Atlantic and Arctic Oceans. In this paper, we apply a coupled ice-ocean model, with extreme atmospheric forcing relevant to the winter AO, to further investigate the possible connections among the winter AO, the North Atlantic water inflow, and winter sea ice and sea water temperature in the Barents Sea. We focus on intraseasonal variations rather than interannual or epochal variations, in contrast to earlier studies that address responses to sustained (several years to decades) AO anomalies (Proshutinsky and Johnson, 1997; Zhang, J. *et al*., 1998; Arfeuille *et al*., 2000; Zhang and Hunke, 2001; Holland *et al*., 2001; Zhang, X. *et al*., 2003).

2. Model description

The sea ice component of the coupled model consists of a thermodynamic model based on a multi-category ice thickness distribution function (Hibler, 1980; Yao *et al*., 2000) and a dynamical model based on a viscous-plastic sea ice constitutive law (Hibler, 1979). The ocean component of the coupled model is taken from the Princeton Ocean Model (Blumberg and Mellor, 1987; Yao *et al*., 2000; Wang *et al*., 2002, 2004). The model uses sigma coordinates with a free surface in the vertical, and employs a mode time-split technique. The ice-ocean coupling process is governed by the boundary processes discussed by Mellor and Kantha (1989). The domain of the coupled model covers the whole Arctic and the northern North Atlantic sector, and its horizontal resolution is 27.5 km. For detailed information about the coupled model, refer to the studies of Yao *et al*. (2000) and Wang *et al*. (2002, 2004). In this study, upper ocean heat content is defined by

$$HT_c = \int_{\text{depth}} \rho C_p (T - T_{\text{ref}}) \mathrm{d}z, \tag{1}$$

where T and T_{ref} (273.15 K) are the ocean temperature and reference temperature; ρ

($1025\,\mathrm{kg\,m^{-3}}$) and C_p ($3903\,\mathrm{J\,K^{-1}\,kg^{-1}\,m^2}$) sea water density and specific heat constant, respectively. The integral is from the surface to 210 m, at the bottom of the halocline (Zhang and Zhang, 2001).

3. Atmospheric forcing

The atmospheric forcing from two extreme regimes defined by the AO index drives the coupled ice-ocean model. We only consider the winter season (January–March) (Thompson and Wallace, 2000). Based on the time series of interannual variations of the winter AO (averaged over three months), we choose from the past several decades those winters for which the AO's standard deviation was >1.0 or <-1.0. The positive

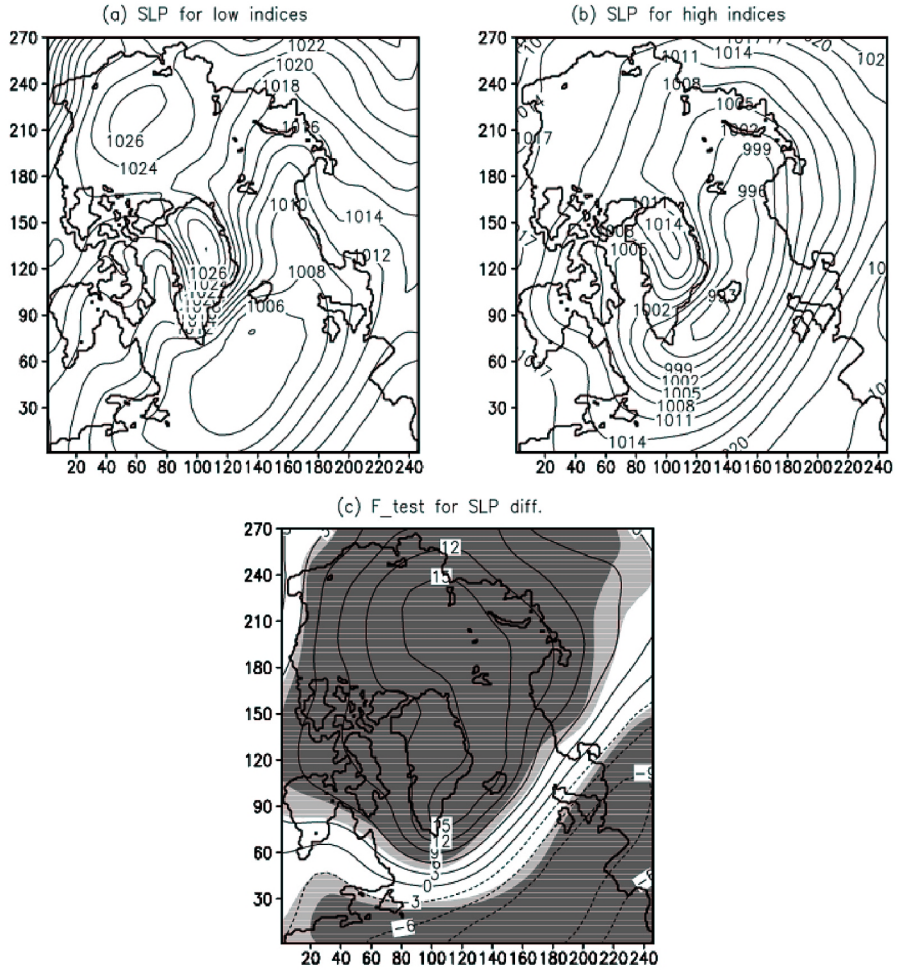

Fig. 1. Composites of the winter mean SLP (a) AO index <-1, (b) AO index >1, and (c) differences (a minus b). The light (dark) represents 0.05 (0.01) confidence level. Contour interval: (a) 2 hPa, (b) and (c) 3 hPa.

phase cases include the winters of 1976, 1967, 1973, 1992, 1993, 1990, 1989; negative phase cases include the winters of 1969, 1960, 1958, 1966, 1970, 1977 (ranked from the minimum to the maximum of the AO). The atmospheric forcing consists of monthly mean surface air temperature (2-m), sea level pressure, surface wind (2-m), and specific humidity and precipitation rate. Grids of these variables are obtained from the reanalysis of the National Centers for Environmental Prediction (NCEP) and the National Center for Atmospheric Research (NCAR) (Kalnay *et al*., 1996). These monthly mean variables are interpolated into daily forcing.

For each year, we ran the coupled model from January 1 to March 31 with the same oceanic initial conditions that were saved after a 36-year spin-up, which includes a 20-year spinup with monthly climatological forcing (averaged over the period of 1958–1998) and a 16-year (1958–1974) integration under monthly forcing.

In order to explain better the model's response to the atmospheric forcing, it is helpful to display how the changes are reflected in the surface atmospheric forcing. To save space, we only show the winter mean condition (averaged over the three months). Considering the important roles of wind-driven motion, we only show the changes in the surface winds and SLP.

During the low phase of the winter AO, there is a weakened Icelandic Low and a concurrent high-pressure center over the Arctic Basin (Beaufort High), with a central pressure above 1025 hPa (Fig. 1a). Correspondingly, there is an anticyclonic circulation anomaly occupying much of the Arctic Basin (Fig. 2a). Strong onshore winds appear over the northern Alaska coast, the Chukchi Sea, and the East Siberian Sea, while the opposite scenario (offshore wind) is apparent over the Kara Sea, the Barents Sea, and the Norwegian coast. Over the western entrance of the Barents Sea, easterlies prevail. During the high phase of the winter AO, the predominant feature is a

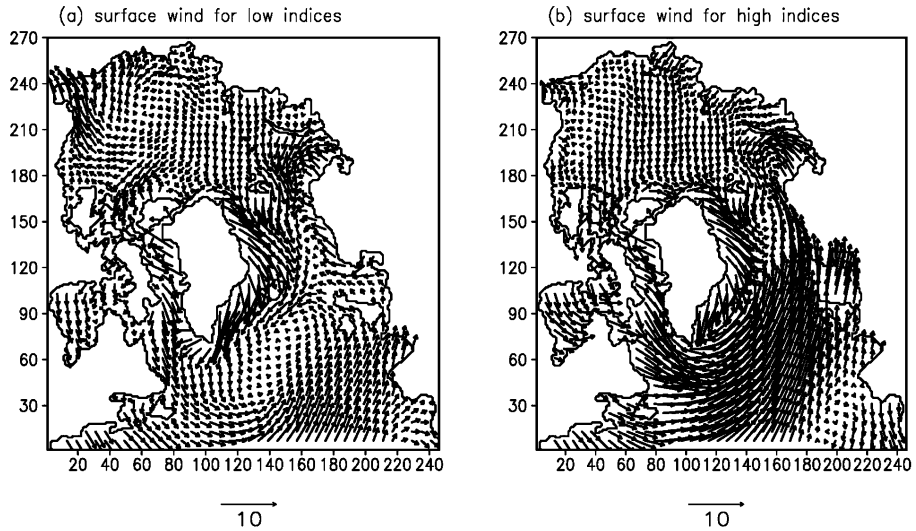

Fig. 2. Composites of the winter mean atmospheric surface wind forcing (a) AO index <-1 and (b) AO index >1, unit: m s^{-1}.

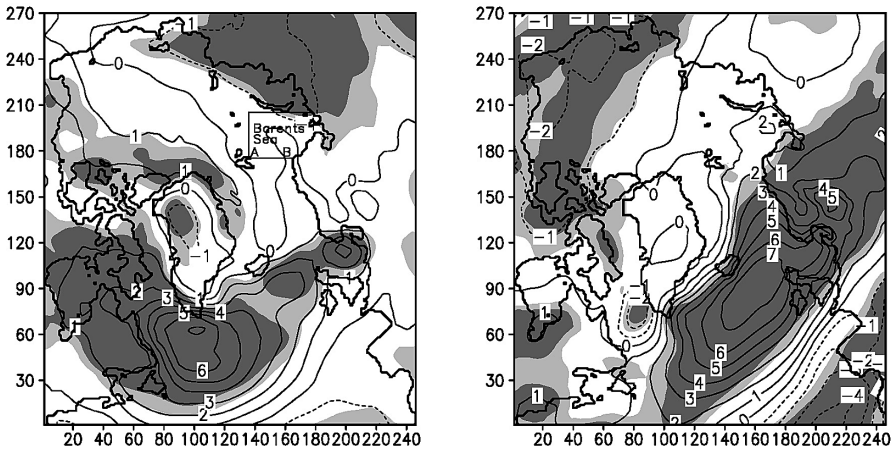

Fig. 3. F-tests for differences in the atmospheric mean (left) u and (right) v component between the two regimes. The light (dark) denotes that differences (the high phase minus the low phase) exceed the 0.05 (0.01) confidence level. The area surrounded by the curve is the Barents Sea; the line segment A and B stands for the western entrance of the Barents Sea.

strengthened and expanded Icelandic Low (Fig. 1b); compared to the low phase of the AO, SLP is lower by up to 15 hPa over the central Arctic Basin and Greenland, Norway, and part of the Barents Sea. Apparently, the Beaufort High has disappeared. An F-test for the mean difference between the two regimes clearly indicates that changes in the SLP over the whole Arctic Basin and the mid-latitudes of the North Atlantic exceed the 0.01 statistical significance level (Fig. 1c). The surface wind fields also change noticeably compared to the low phase of the AO (Fig. 2b), as enhanced airflow across mid-latitudes of the North Atlantic expands northeastward to the Barents Sea. Over the Barents, Kara, and Laptev Seas, the offshore wind becomes even more robust, compared to Fig. 2a. Over the Arctic Basin, the circulation does not show strong coherence.

Although the changes of SLP are significant over the whole Arctic, corresponding changes in wind fields are not significant (Fig. 3) over the central Arctic Basin, and much of the Barents, and Greenland Seas. Yet the differences of wind forcing are highly significant over the ocean areas from which ocean currents flow northeastward to the Barents Sea (Fig. 3 right).

4. Model response

We focus our attention on the Barents Sea (Fig. 3 left) and choose a horizontal-depth section along the western entrance of the Barents Sea (see section A-B in Fig. 3 left) to examine the relationship between the AO and the North Atlantic water inflow into the Barents Sea. Figure 4 shows the interesting result that the enhanced relationship is observed only during the AO's positive phases. The most significant positive correlations overlay the continental shelf. This implies that the low phase of the winter AO has little immediate influence on the North Atlantic water inflow into the Barents

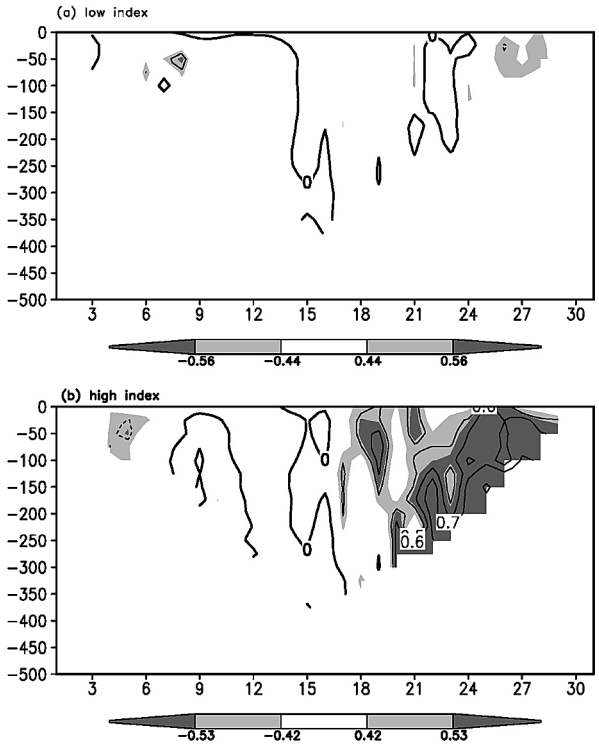

Fig. 4. Correlations of the monthly mean AO index with the normal current velocity across the western entrance of the Barents Sea: (a) low phase periods and (b) high phase periods. The area with the light (dark) indicates that correlations exceed the 0.05 (0.01) confidence level. Contours: 0.0, 0.5, 0.6, 0.7.

Sea, at least on a monthly timescale. Consequently, the high phase of the winter AO drives more North Atlantic water inflow to the Barents Sea. As a compensation, there will be more sea ice and freshwater export out of the Arctic Basin through Fram Strait because the weakened Beaufort Gyre releases fresh water and sea ice to the North Atlantic (Proshutinsky *et al*., 2002).

We calculate monthly mean sea ice area and volume in the Barents Sea. It is found that there is a high correlation between sea ice area and volume ($r=0.82$). In addition, there is a significant negative correlation of -0.7 (-0.45) between the North Atlantic water net inflow and sea ice area (volume), which is consistent with previous studies (Dickson *et al*., 2000; Wu *et al*., 2000). Consequently, the enhanced net inflow of warmer Atlantic water into the Barents Sea causes decrease of sea ice. Compared to the heat content for the low phase of the winter AO (Fig. 5a), the positive phase causes increases in upper ocean heat content in the eastern Greenland-Norwegian-Barents Seas, with its maximum positive anomalies exceeding 0.8×10^8 J (Fig. 5b). Meanwhile, strong heat content negative anomalies occupy the Baffin Bay-Labrador Sea and the North Atlantic south to Iceland (Fig. 5b). Apparently, the spatial distribution of upper ocean heat content anomalies shows a strong seesaw structure in the North

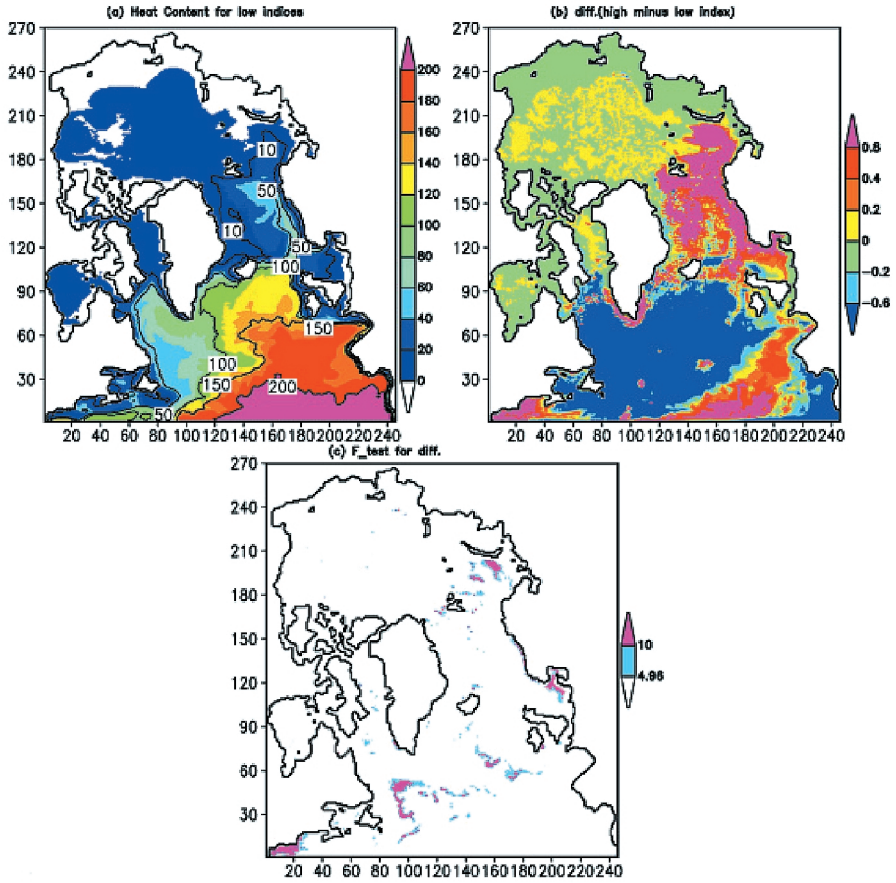

Fig. 5. Composites of the winter mean upper heat content (a) the positive phase of the AO, (b) differences of the heat content (the positive phase minus the negative phase), and (c) F-test for differences of the heat content, In (c), the color bar stands for upper ocean heat content differences exceeding the 0.05 and 0.01 confidence levels, respectively. Contours: (a) 10, 50, 100, 150, 200. Unit: $\times 10^8$ J.

Atlantic-Nordic and Barents Seas. A significance test for differences of heat content between the positive and the negative phase of the winter AO also confirms that changes of upper ocean heat content are significant only in the Labrador and Barents Seas (Fig. 5c). As can be seen (Fig. 5c), no significant changes in heat content can be found in the Arctic Basin and the Siberian marginal seas.

Figure 6 shows a horizontal-depth section of sea water temperature and sea water temperature difference (the positive minus the negative phase of the winter AO) along the western entrance of the Barents Sea. It is clear that the North Atlantic water with high temperature mainly appears in the bottom and the vicinity of the Norwegian shelf with cool water overlying it during the low phase of the winter AO (Fig. 6a). The warmest North Atlantic water appears near a depth of 100 m beneath the surface. During the high phase of the winter AO, apparent warming occurs in the subsurface,

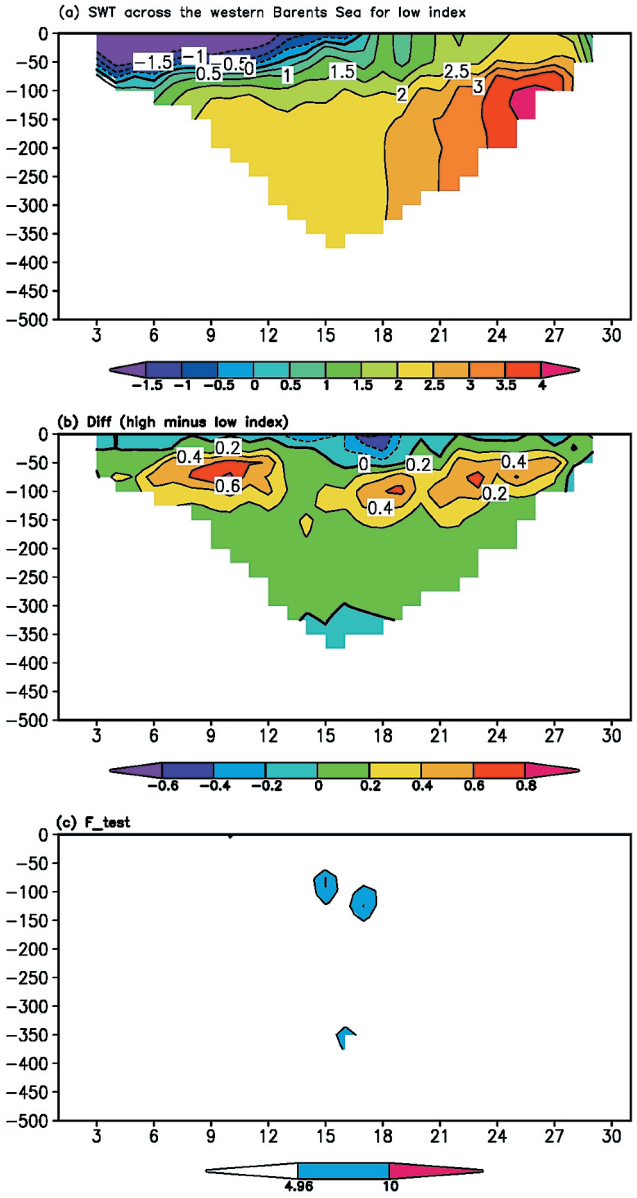

Fig. 6. A horizontal-depth section of composite of variables along the western entrance of the Barents Sea: (a) the winter monthly mean water temperature during the low phase of the winter AO, (b) differences in mean water temperature between the two regimes (the high phase minus the low phase), and (c) F-test for mean water temperature difference. In (c), the blue and magenta area stands for water temperature differences exceeding the 0.05 and 0.01 confidence levels, respectively.

with concurrent cooling above (Fig. 6b). This indicates that significant warming in the Barents Sea occurs below the surface rather than at the surface. An F-test for temperature differences further supports this conclusion (Fig. 6c). Generally speaking, the ocean upper layer responds to wind forcing by flowing to the right of the direction of air motion. Winter anticyclonic flow drives the upper water to the center of the circulation, raising its sea level during the low phase of the winter AO. During the high phase of the winter AO, the atmospheric anticyclonic forcing is weaker than normal; thus, the Beaufort Gyre is weaker, and cold fresh water and sea ice are released to the

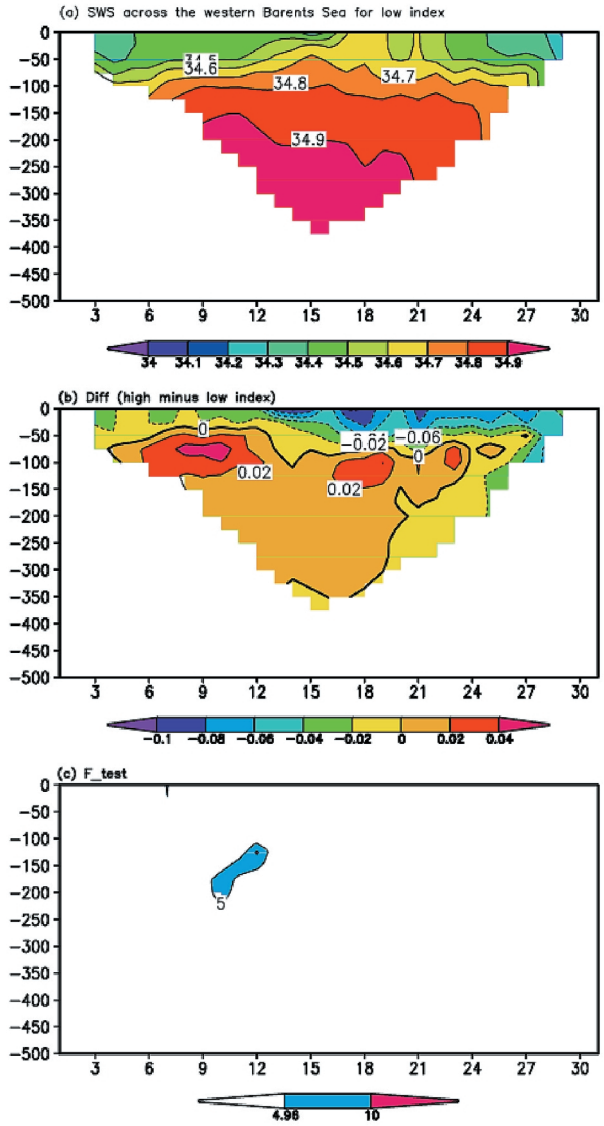

Fig. 7. Same as Fig. 6 except for salinity

Greenland and Barents Seas (Proshutinsky *et al*., 2002). Consequently, the upper layer in those sea regions tends to be lower temperature than normal. Simultaneously, the positive phase of the AO drives more North Atlantic warm water into the Barents Sea. This may be the reason why surface cooling occurs companied with subsurface warming.

Compared to distributions of salinity during the low phase of the winter AO, salinity also increases below the surface, with fresh water overlying it during the high

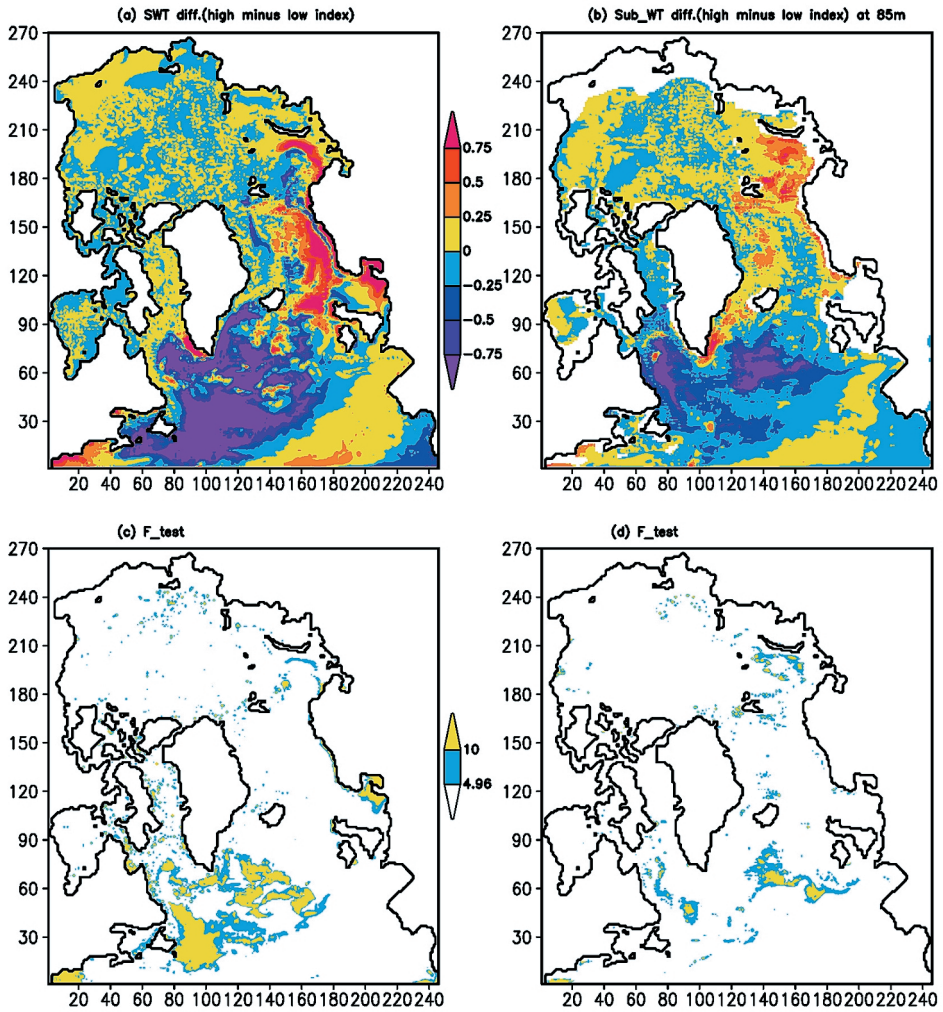

Fig. 8. (a) The difference in the mean surface water temperature between the two regimes (the high phase minus the low phase), (c) F-tests for differences in the mean surface water temperature between the two regimes; (b) and (d) are the same as (a) and (c), respectively, except at the depth of 85 m. In (c) and (d), the blue and yellow areas indicates that the water temperature difference between the two regimes exceeds the 0.05 and 0.01 confidence levels, respectively.

phase of the AO (Fig. 7). Compared to the low phase of the winter AO, surface water temperature in the high phase decreases in the western and central Barents Sea, with concurrent warming in the eastern and southeastern Barents Sea (Fig. 8a). However, in the subsurface layers, the warming is apparent in the whole Barents Sea during the high phase of the winter AO (Fig. 8b). A significance test (F-test) supports this conclusion (Figs. 8c, d). As can be seen (Fig. 8c), significant surface temperature differences appear in the south of Greenland, *i.e.*, the Labrador Sea and parts of the North Atlantic. However, in the Norwegian Sea, Barents Sea, and the Arctic Ocean, there are only small areas where surface temperature differences are significant. In the subsurface layer (Fig. 8d), the shaded area is apparently diminished in the Baffin Bay-Labrador Sea, but extended in the Barents Sea.

The positive phase of the winter AO drives more North Atlantic water inflow into the Barents Sea. Simultaneously, as a compensation, it is also responsible for more fresh water and sea ice export out of the Arctic Basin via Fram Strait and the northern Barents Sea. As can be seen (Fig. 9), compared to the distribution of sea ice concentration during the low phase (Fig. 9a), the high phase of the winter AO causes decrease of sea ice concentration in the eastern and southeastern Barents Sea, with concurrent apparent increases in the central Barents Sea and the Baffin Bay-Labrador Sea (Fig. 9b). Changes in sea ice thickness in the Barents Sea also show similarity to those of sea ice concentration (not shown). It is well known that the major part of the fresh water and sea ice export from the Arctic Ocean takes place through Fram Strait. A minor export of sea ice and fresh water occurs through the Barents Sea. Most of the ice efflux from the Arctic Ocean to the Barents Sea melts there. This may be the reason why cooling and low salinity surface water appear in the central and western Barents Sea during the positive phase of the winter AO (Figs. 6 and 7).

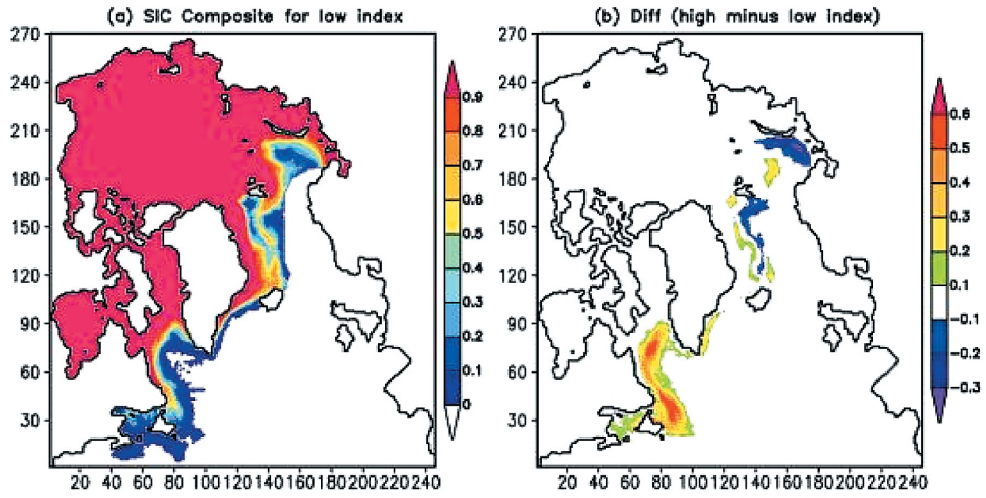

Fig. 9. (a) Sea ice concentrations for the low phase of the winter AO, (b) Differences of sea ice concentrations (the high phase minus the low phase).

5. Observational evidence

To further confirm the subsurface warming in the Barents Sea predicted by the ice-ocean model, we analyzed the historical hydrological data set. For the Barents Sea, we used data for the period of 1898–1993 from the National Oceanographic Data Center (NODC, 1998). Due to sparsity of the data set, we selected the available water temperature data for the high AO phase (1967, 1973, 1976, 1989, 1990) and for the low AO phase (1955, 1958, 1960, 1966, 1970, 1977). Again, due to data sparsity in depths,

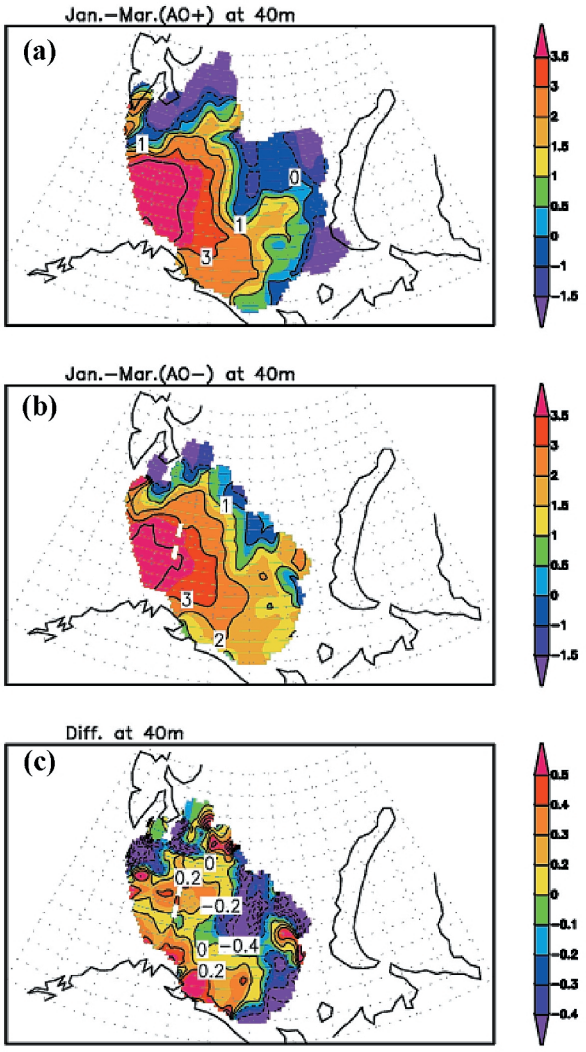

Fig. 10. Composites of the winter (Jan. to Mar.) subsurface water temperature (40-m) in the Barents Sea, (a) the high phase, (b) the low phase, and (c) differences (a minus b), unit: °C.

particularly below 50 m, the composite of temperature for both phases were calculated only at 40 m (Fig. 10). Comparing Fig. 10a with Fig. 10b, the positive phase of the AO is accompanied by subsurface cooling in the central and eastern Barents Sea, which can be attributed to more cold fresh water and sea ice export into the Barents Sea compared to during the negative phase of the AO. The difference map of the temperature shows positive temperature anomalies around the southern and southwestern Barents Sea (Fig. 10c). Therefore, the subsurface warming predicted by the model is consistent with the observations.

6. Conclusions

Using a coupled ice-ocean model, we investigated possible connections of the winter AO (Jan.–Mar.) with Atlantic warm water inflow, sea water temperature, and sea ice in the Barents Sea on a monthly time scale. Based on the time series of interannual variations in the winter AO index, we chose those winters in which standard deviations of the winter mean AO indices were >1.0 or <-1.0 as cases of extreme atmospheric forcing. For each experiment, we ran the model from January 1 to March 31 with the same oceanic initial conditions. The following conclusions can be drawn about relationships on a monthly time scale:

(1) The winter AO shows significant positive correlations with the North Atlantic water inflow into the Barents Sea only during the high phase of the winter AO.

(2) Compared with the low phase of the winter AO, the high phase leads to the most significant warming appearing below the surface rather than at the surface in the Barents Sea. Correspondingly, the high phase of the winter AO results in decreases in the surface temperature rather than increases in most of the Barents Sea because of enhanced export of sea ice from the Arctic Ocean to the Barents Sea, where it melt.

(3) As response to the winter AO forcing, changes in the upper oceanic heat content display a seesaw structure in the North Atlantic-Nordic and Barents Seas.

Acknowledgments

We thank the International Arctic Research Center–Frontier Research System for Global Change and IARC/CAMP Project for financial support. B. Wu and R. Zhang also are grateful to the National Nature Science Foundation of China (grant No. 40225012) for financial support. The first author is grateful to Prof. John E. Walsh and Dr. M. Jin for constructive discussions.

References

Alexander, M., Bhatt, U., Walsh, J., Timlin, M., Miller, J. and Scott, J. (2004): The atmospheric response to realistic Arctic sea ice anomalies in an AGCM during winter. J. Climate, **17**, 890–905.

Arfeuille, G., Mysak, L.A. and Tremblay, L.B. (2000): Simulation of the interannual variability of the wind-driven Arctic sea-ice cover during 1958–1998. Climate Dyn., **16**, 107–121.

Blumberg, A.F. and Mellor, G.L. (1987): A description of a three-dimensional coastal ocean circulation model. Three-Dimensional Coastal Ocean Models, ed. by N.S. Heaps. Washington, D.C., Am. Geophys. Union, 1–16.

Deser, C., Magnusdottir, G., Saravanan, R. and Phillips, A. (2004): The effects of North Atlantic SST and sea ice anomalies on the winter circulation in CCM3. Part II: Direct and indirect components of the response. J. Climate, **17**, 877–889.

Dickson, R.R., Osborn, T.J., Hurrell, J.W., Meincke, J., Blindheim, J., Adlandsvik, T., Vinje, G., Alekseev, G. and Maslowski, W. (2000): The Arctic Ocean response to the North Atlantic Oscillation. J. Climate, **13**, 2671–2696.

Gao, D.-Y. and Wu, B.-Y. (1998): A preliminary study on decadal oscillation and its oscillation source of sea-ice-air system in the Northern Hemisphere. Polar Meteorol. Glaciol., **12**, 68–78.

Häkkinen, S. and Geiger, C.A. (2000): Simulated low-frequency modes of circulation in the Arctic Ocean. J. Geophys. Res., **105** (C3), 6549–6564.

Hibler, W.D., III (1979): Dynamic thermodynamic sea ice model. J. Phys. Oceanogr., **9**, 815–846.

Hibler, W.D., III (1980): Modeling a variable thickness sea ice cover. Mon. Weather Rev., **108**, 1943–1973.

Holland, M.M., Bitz, C.M., Eby, M. and Weaver, A.J. (2001): The role of ice-ocean interactions in the variability of the North Atlantic thermohaline circulation. J. Climate, **14**, 656–675.

Ikeda, M. (1990): Decadal oscillations of the air-ice-ocean system in the Northern Hemisphere. Atmosphere-Ocean, **28**, 106–139.

Kalnay, E. and coauthors (1996): The NCEP/NCAR 40-year Reanalysis Project. Bull. Am. Meteorol. Soc., **77**, 437–471.

Mellor, G.L. and Kantha, L. (1989): Ice-ocean coupled model. J. Geophys. Res., **94** (C8), 10937–10954.

Proshutinsky, A.Y. and Johnson, M.A. (1997): Two circulation regimes of the wind-driven Arctic Ocean. J. Geophys. Res., **102** (C6), 12493–12514.

Proshutinsky, A., Bourke, R.H. and McLaughlin, F.A. (2002): The role of the Beaufort Gyre in Arctic climate variability: Seasonal to decadal climate scales. Geophys. Res. Lett., **29** (23), 2100, doi: 10.1029/2002GL015847.

Thompson, D.W.J. and Wallace, J.M. (2000): Annular modes in the extratropical circulation. Part I: Month-to-month variability. J. Climate, **13**, 1000–1016.

Wang, J., Liu, Q. and Jin, M. (2002): User's guide for a coupled ice-ocean model (CIOM) of the Pan-Arctic and North Atlantic Oceans. IARC-FRSGC Report, No. 2002–01, University of Alaska Fairbanks.

Wang, J., Liu, Q., Jin, M., Ikeda, M. and Saucier, F. (2004): A coupled ice-ocean model in the pan Arctic and the northern North Atlantic Ocean: Simulation of seasonal cycles. published by J. Oceanogr.

Wu, B.-Y., Huang, R.-H. and Gao, D.-Y. (2000): Arctic sea ice bordering on the North Atlantic and interannual climate variations. Chinese Sci. Bull., **45** (18), 1993–1997 (in Chinese).

Wu, B.-Y., Wang, J. and Walsh, J. (2004): Possible feedback of winter sea ice in the Greenland and the Barents Sea on the local atmosphere. Mon. Weather Rev., **132**, 1868–1876.

Yao, T., Tang, C.L. and Peterson, I.K. (2000): Modeling the seasonal variation of sea ice in the Labrador Sea with a coupled multicategory ice model. J. Geophys. Res., **105** (C1), 1153–1165.

Zhang, J., Rothrock, D.A. and Steele, M. (1998): Warming of the Arctic Ocean by a strengthened Atlantic inflow: Model results. Geophys. Res. Lett., **25**, 1745–1748.

Zhang, X. and Zhang, J. (2001): Heat and freshwater budgets and pathways in the Arctic Mediterranean in a coupled ocean/sea-ice model. J. Oceanogr., **57**, 207–234.

Zhang, X., Ikeda, M. and Walsh, J.E. (2003): Arctic sea ice and freshwater changes driven by the atmospheric leading mode in a coupled sea ice-ocean model. J. Climate, **16**, 2159–2177.

Zhang, Y. and Hunke, E.C. (2001): Recent Arctic change simulated with a coupled ice-ocean mode. J. Geophys. Res., **106** (C3), 4369–4390.